J. Fluid Mech. (1990), *vol.* 217, *pp.* 349–366
Printed in Great Britain

Radial migration of a single particle in a pore by the resistive pulse and the pressure reversal technique

By LARS INGE BERGE
Department of Physics, University of Oslo, PO Box 1048 Blindern, 0316 Oslo 3, Norway

(Received 10 April 1989 and in revised form 29 August 1989)

Radial migration (particle motion transverse to streamlines) in a system which combines frequent entry, straight pore, and exit regions were investigated experimentally for small particle and pore sizes. Pore diameters were less than 30 μm and typical particle to pore diameter ratios were about 0.25. Our new modification of the resistive pulse technique based on pressure reversal, extends this experimental technique to also include single-particle flow dynamics. By pressure drive, a particle in an electrolyte enters a current-carrying pore and an increase in resistance proportional to the particle volume is detected. When the particle exits the pore, the pressure can be reversed such that the particle re-enters the pore. Detailed studies of particle flow properties in a size range relevant to flow in porous media is now possible. The emphasis in this investigation is on radial migration. The effect of particle sedimentation has been negligible, while particle diffusion becomes significant for submicron particles. The measured evolution of the transit time as the particle migrates compares well with an empirical relationship for the migration velocity first proposed by Segré & Silberberg (1962*a*, *b*) and later verified by Ishii & Hasimoto (1980). Entrance and exit effects do not seem to be important for long pores, the results scale very nicely when the pore length is changed.

1. Introduction

Radial migration is the tendency of particles in Poiseuille flow to move radially across streamlines towards an equilibrium position somewhere between the tube axis and the wall. Segré & Silberberg (1962*a*, *b*) studied the radial particle displacement in dilute suspensions of neutrally buoyant rigid spheres in Poiseuille flow and made the remarkable observation that the spheres migrated slowly into a thin annular region about 0.6 tube radii from the axis, irrespective of the radial position at which the spheres first entered the tube. Similar observations were made by Oliver (1962), who also studied the influence of particle rotation on radial migration in Poiseuille flow and concluded that the equilibrium position is closer to the axis when the spheres are prevented from rotating. Karnis, Goldsmith & Mason (1966) measured how the equilibrium position shifts closer to the axis when the particle diameter is increased. Experiments by Aoki, Kurosaki & Anzai (1979) in a vertical tube have clarified the influence of the relative particle–fluid velocity on the equilibrium position, which can be shifted continuously from the wall to the axis by varying the density difference between the particle and the fluid. The equilibrium position is shifted towards the axis if the particle lags behind the flow and towards the wall for particles preceding the flow.

It was early pointed out by Saffman (1956), Brenner & Happel (1958), and Bretherton (1962) that no sideways force on a single rigid spherical particle can be derived without considering the inertial effects, represented by the nonlinear terms in the Navier–Stokes equations. Rubinow & Keller (1961) obtained a sideways force by considering a Magnus-type effect, but their theory was later shown to be inapplicable to radial migration (Saffman 1965). Owing to the mathematical complexity of the problem, the rate of theoretical progress has been slow. A solution to the migration problem for a small sphere in a circular tube was eventually obtained by Ishii & Hasimoto (1980) and their results agree well with known experiments. For a neutrally buoyant particle, they obtained a stable equilibrium position at 0.71 tube radii from the axis and an unstable equilibrium position at the axis.

Experimental investigations on radial migration have been performed using different experimental techniques and typical particle and tube diameters have been in the millimetre and centimetre range and the tube has been vertical. Segré & Silberberg (1962*a*) designed an apparatus based on the simultaneous blocking out of two mutually perpendicular light beams by a particle passing through their common region. Karnis *et al.* (1966) followed the particle trajectory with a travelling microscope, while Jeffrey & Pearson (1965), Tachibana (1973), and Aoki *et al.* (1979) used photographic methods. We present measurements using a new experimental approach (Berge, Feder & Jøssang 1989) which allows studies in a size range which hitherto has been difficult to access, tube (pore) diameters were less than 30 μm. This investigation was motivated by our interest in the physics of porous media and in order to study flow properties in microscopic pores, the effect of radial migration is important.

The resistive pulse technique is probably the most widespread method for counting and sizing particles. The invention of a means for counting and sizing particles suspended in a conducting fluid was patented by Coulter (1953) and his invention has become commercially available with the designation Coulter Counter. The increase in resistance is measured when single particles are transported through a current-carrying pore. The resulting pulses have, if the pore is sufficiently long, a well-defined height, form, and width. These parameters are related to particle volume, shape, and transit time. We have extended the resistive pulse technique to obtain information about flow dynamics in single pores of sizes relevant to flow in porous media. Every time a particle exits the pore, the pressure is reversed and the particle re-enters the pore. In this way, a relatively short pore may be used to approximate experimentally the flow behaviour in an effectively infinite long pore. However, since the particle exits the pore between reversals, effects outside as well as inside the pore can be studied. Our system may be considered as a one-dimensional porous medium with only one pore size. To our knowledge, this is the first time such measurements have been performed and they represent a new and unexplored potential of the resistive pulse technique. In this paper, we demonstrate how the pressure reversal technique enables us to obtain very detailed information about single-particle flow dynamics by measuring the transit times of a single particle flowing back and forth through a pore. We have studied radial migration of single polystyrene spheres flowing through horizontal pores with diameters about 3 and 30 μm. Our measurements compare well with theory and previous measurements on a larger scale in long tubes. Section 2 briefly describes our experimental set-up and the basic features of the resistive pulse technique, including the pressure reversal technique. Section 3 relates the particle

transit time through the pore to the radial migration velocity. Our measurements are discussed and compared with theoretical predictions in §4.

2. Experimental

2.1. *Pores and solution*

The experiments have been carried out using three different pores. Two glass capillaries with diameters 27 and 30 μm and resistive lengths 540 and 315 μm, respectively, have been made by drawing down lengths of capillary tubing and then grinding thin slices with the required diameter until the desired length is obtained. The other pore has been made at General Electric Corporate Research and Development (Schenectady, New York) in cast polycarbonate by the Nuclepore (etched particle track) process, see Fischer & Spohr (1983). The pore diameter is 3.1 μm and its resistive length 9.5 μm. To make a correction for end effects, the resistive pore length should be used instead of the geometrical pore length. The resistive pore length exceeds the geometrical pore length by approximately 0.8 times the pore diameter (DeBlois & Bean 1970). The cross-sections of all pores are very closely circular.

The basic electrolyte used was 0.01 M Tris (pH 7.4) in 0.15 M NaCl and 0.02% Tween (Sigma P-1379). Tween is used to prevent later particle coagulation and pore plugging. The solution was filtered through a 0.22 μm Millipore filter before adding monodisperse polystyrene spheres (Dynospheres, Dyno Industries, Oslo, Norway and Dow-Latex, Serva, Feinbiochemica, Heidelberg, Germany), 0.8 μm diameter spheres for the small pore and 7.1 μm diameter spheres for the large pores. The particle density is 1.044 g/cm^3. For the 3.1 μm diameter pore, the effect of sedimentation is negligible owing to the small particle size used. For measurements using the larger pores, approximately 10 wt % sucrose was added to the basic electrolyte to match the particle density and to avoid the uncertainty caused by sedimentation. In addition to increasing the density, the addition of sucrose also increases the viscosity.

2.2. *Experimental arrangement*

The complete experimental arrangement is shown schematically in figure 1 and the various parts of the set-up will be described briefly. A horizontal microscopic pore connects the two chambers of the experimental Plexiglas cell. Finished capillary sections are epoxy glued to Plexiglas disks with 1.7 cm outer diameter and a small central hole. A disk containing a pore is mounted between the two halves of the experimental cell using viton O-rings. The volume of each chamber is approximately 1 cm^3 and they are filled with a conducting fluid, in which the particles to be analysed are suspended. Each chamber has a filling and pressure tube leading to it and contains a silver, silver chloride electrode connected to a constant voltage source (1.22 or 2.47 V). A pressure difference across the pore sets up a hydrodynamic flow. The cell is placed on a vibration damped table in a brass box that provides shielding against electrical interference.

When a particle enters the pore, the resistance between the electrodes increases and consequently there is a current drop, which is amplified using a Keithley Model 427 Current Amplifier with a voltage output and a minimum rise time of 15 μs. The output signal is connected to a DATA 6000 waveform analyser (Data Precision Corp. USA), which displays an electrical pulse on a CRT screen when a particle passes through the pore. DATA 6000 is equipped with a 100 kHz plug-in module which

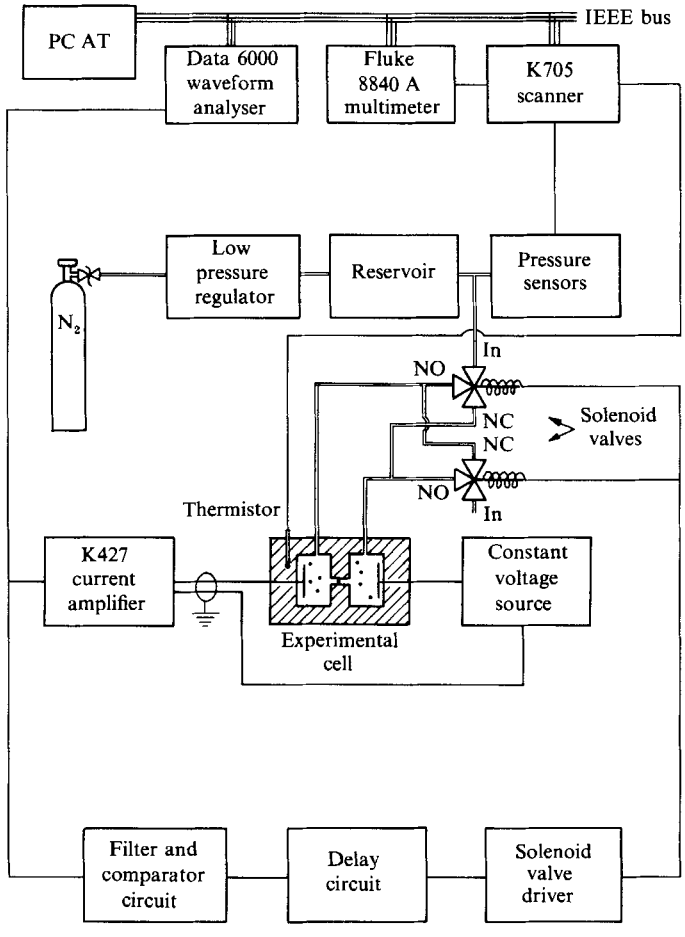

FIGURE 1. Complete schematic experimental arrangement. The experimental cell connected to a constant voltage source and a current amplifier is the heart of our system. A low-pressure regulator maintains a constant pressure in the reservoir. A trigger signal to the solenoid valves controlling pressure reversal is derived from the particle pulses. The outputs of the valves are labelled NO (normally open) and NC (normally closed). The signal from the current amplifier is analysed with a waveform analyser. Pressure is measured with differential pressure sensors and the temperature of the cell is measured with a thermistor. The instruments are IEEE-488 interfaced to a personal computer.

offers a minimum sampling period of 10 μs and a rise time of 7 μs and the instrument computer offers advanced signal processing capabilities. The pressure drop across the pore is measured with a differential pressure sensor (voltage output) and the temperature with a thermistor (resistance output). A Keithley Model 705 Scanner and a Fluke 8840A Multimeter are used for reading pressure and temperature. The instruments are IEEE-488 interfaced to a COPAM PC-501 TURBO computer through a TECMAR PC-MATE interface card.

2.2.1. *Pressure reversal technique*

The pressure reversal technique requires that there is a pressure drop across the pore which sets up a hydrodynamic flow to transport particles through the pore. The schematic experimental arrangement for pressure reversal is included in figure 1. In

our system, we may reverse the pressure shortly after a particle has exited the pore and the particle is forced to flow back through the pore. By reversing the pressure every time a particle has exited the pore, dynamics of single particles may be studied over long periods of time. If the particle is reversed at moderate frequencies, the flow in the pore will have reached a steady state before the particle re-enters the pore. By symmetry, the two flow directions are equivalent if the pore is horizontal and this is also observed experimentally. Hence, when it comes to radial migration, a relatively short pore may be used to approximate experimentally the motion of a single particle in a much longer pore, effectively in an infinite long pore.

By using two miniature solenoid three-way valves (LFAA 1200118H, The Lee Co.) connecting the chambers of the experimental cell to the pressure supply and to atmospheric pressure as indicated in figure 1, the pressure drop across the pore may be reversed at regular short-duration intervals. The two valves are coupled in the same mode. In the unenergized mode, the NO (normally open) outlet is connected to the cell. A 12 V d.c. voltage applied to the coil is required to energize the valves and switch the inlet pressure to the NC (normally closed) outlet.

A trigger signal is used to change the mode of the valves for reversing the pressure. The trigger signal is derived from the particle pulses by the aid of a trigger circuit, which comprises a filter and comparator circuit, a delay circuit, and a solenoid valve driver circuit shown schematically in figure 1. The filter and comparator circuit is supplied with a passband filter (0.2–2 kHz) and a discriminator (0–1 V) to select the signal of interest. The trigger mode is switched every time a negative transition in the pulse signal (corresponding to a particle exiting the pore) crosses the discriminator level. The delay circuit provides the opportunity to delay the transitions of the trigger signal and the time the particle spends outside the pore between reversals is therefore adjustable. The solenoid valve driver circuit makes the trigger signal compatible with the requirements of the solenoid valves.

The pressure supply is compressed nitrogen from a tank. The gas is filtered and reduced to a maximum of 8 bar before entering the inlet of a Norgren 11-818-999 low-pressure regulator connected to an external reservoir of 1 litre. For every pressure reversal, the tube connections from one valve to the cell have to be vented, resulting in a small loss of gas ($\sim 0.05\,\%$) from the reservoir. The Norgren regulator maintains a constant average pressure in the reservoir.

Our version of DATA 6000 may at most continuously record 3 transit times per second. In order to measure the transit time at regular intervals, the time between reversals must be set correctly. In the present study, the time a particle spends outside the pore between reversals has been either 250 or 500 ms which corresponds to measuring every second and every transit time. The particle transit time through the pore has been in the range from 0.2 to about 20 ms. The low frequency of pressure reversal has been chosen such that DATA 6000 can record every transit time. The high-frequency range is more difficult to handle experimentally and it has so far not been pursued. Two consecutive pulses from a reversed rigid 7.1 μm diameter sphere in a 27 μm diameter and 540 μm long pore are shown in figure 2. The transit time is taken to be the pulse width at half the pulse amplitude.

In order for the pressure reversal technique to function properly, some requirements must be met. The electrodes must exhibit a stable baseline. A large drift will cause the trigger circuit to malfunction. The signal to noise ratio must be sufficient to eliminate malfunction. For long pores, we must therefore use large particles. The particle concentration must be kept low. At large concentrations, a trapped particle is easily lost owing to interactions with other particles.

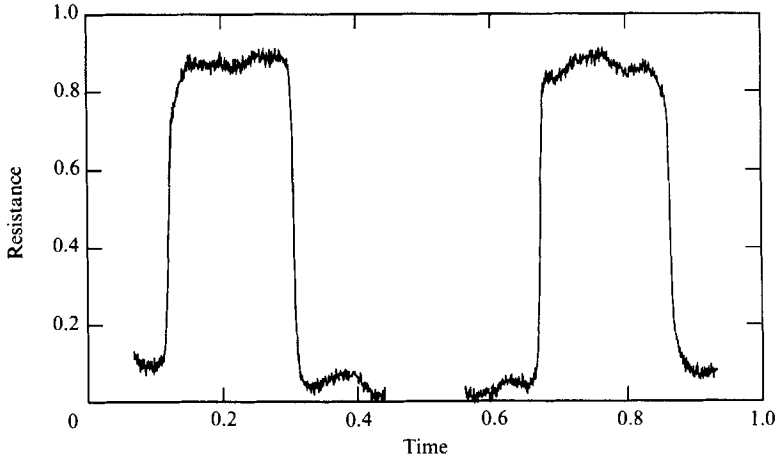

FIGURE 2. Two consecutive reversed pulses from a 7.1 μm diameter sphere flowing back and forth through a 27 μm diameter and 540 μm long pore (unspecified units of time and resistance). The pulse height was 600 Ω and the pulse width about 6.2 ms.

2.3. *Response of the particle analyser*

The basis for the resistive pulse technique is the resistance pulses which are detected every time a particle enters the pore. The pulses may be analysed in terms of height, form, or width. There is no simple solution to the problem of determining the resistance increase of a conducting circular cylinder caused by inserting an insulating sphere far from the ends. Maxwell (1904) obtained an expression for the effective resistivity of a dilute suspension of small insulating spheres in a solution of known resistivity which is applicable to our system. However, in many practical applications, the particle size range of interest extends beyond the validity of Maxwell's expression. Smythe (1964) has analysed the problem of flow around a spheroid in a circular tube in series form. He presents accurate numerical calculations for spheres with values of d/D up to 0.95, where D and d are pore and sphere diameter, respectively. The relative increase in resistance due to the presence of a sphere inside the pore may be given by the Maxwell expression to first order with a size correction factor $S(d/D)$ based on the calculations of Smythe. Thus, the response for our instrument may be expressed as follows:

$$\Delta E = \frac{EG}{R_e}\left(\frac{2V}{3vS(d/D)}+1\right)^{-1}. \tag{1}$$

Here ΔE is the measured voltage change at the output of the current amplifier due to the presence of a sphere of volume v inside a pore of volume V. Further, E is the constant voltage across the pore, G is the current amplifier gain (volts/ampere), and R_e is the pore resistance in the absence of particles.

Before a pore can be used for analysing particles, the pore dimensions must be determined. The electrolyte resistivity and the pore resistance are measured. Then we let spheres of known size pass through the pore one at a time and the corresponding voltage pulses are recorded. Consequently the pore dimensions may be found. Having calibrated the pore, we are able to measure the size of particles passing through the pore. This has been the main use of instruments based on the resistive pulse technique. Or, as will be the concern of this paper, we may relate the measured pulse width to the motion of a particle through the pore.

3. Expression for the particle transit time

The transit time for a particle which is transported through a pore of resistive length L is the quantity which is experimentally obtainable. The transit time is mainly determined by hydrodynamic fluid flow and by radial migration of particles. Since an electric field is applied across the pore, both electro-osmosis and electrophoresis (Dukhin 1974) may contribute to the transit time. Electro-osmosis is induced if the pore is charged. The charged mobile liquid at the interface moves in response to the applied electric field. Owing to internal friction in the liquid, all the liquid in the bulk soon flows with a constant electro-osmotic velocity v_e. Similarly, charged particles suspended in the liquid move in response to the electric field with an electrophoretic velocity v_f. Note that v_e and v_f are functions of pH with a zero value at the isoelectric point, which is material dependent. The electro-osmotic velocity decreases as the inverse square of the pore diameter (DeBlois, Bean & Wesley 1977). In this investigation, electrokinetic effects have been negligible except at low pressure measurements using the 3.1 μm pore. However, in the size range of current interest it is important to be aware of these effects. One way to determine the electrokinetic contribution to the flow is simply to measure the difference in the particle transit time for opposite flow directions for a reversed particle which has reached the equilibrium position.

A schematic figure of a pore with coordinates and relevant parameters is shown in figure 3. The fractional distance from the axis is $x = r/R$, where r is the radial coordinate and R is the pore radius. The coordinate along the pore axis is z, measured from the pore entrance. The particle velocity in the z-direction is $V_p(x)$, and $v_r(x)$ is the radial migration velocity towards the equilibrium trajectory x^*. The maximum Poiseuille fluid velocity is V_m, and V_e is the electrokinetic velocity, the vector sum of the electro-osmotic fluid velocity in the pore and the electrophoretic particle velocity.

The relative importance of inertial to viscous effects depends on the following two Reynolds numbers (Brenner 1966):

$$Re = \frac{\rho_f R V_m}{\eta} = \text{pore Reynolds number}, \tag{2}$$

$$Re_p = \frac{2\rho_f b|V_r|}{\eta} = \text{particle Reynolds number}, \tag{3}$$

where ρ_f is the fluid density, η is the viscosity, b is the particle radius, and V_r is the axial relative velocity between the fluid and the particle.

The transit time is determined by the particle velocity $V_p(x)$,

$$\tau = \int_{z=0}^{L} \frac{dz}{V_p(x)}. \tag{4}$$

According to Smith (1960), an inlet length $\tilde{\lambda} = 0.13 R\,Re$ must be allowed for before Poiseuille flow is established. At low pore Reynolds numbers, the inlet length will be small compared to the pore length. It is assumed that the fluid entering the pore immediately settles into the laminar parabolic flow pattern. The equilibrium transit time for a particle travelling along the equilibrium trajectory will be denoted τ^*.

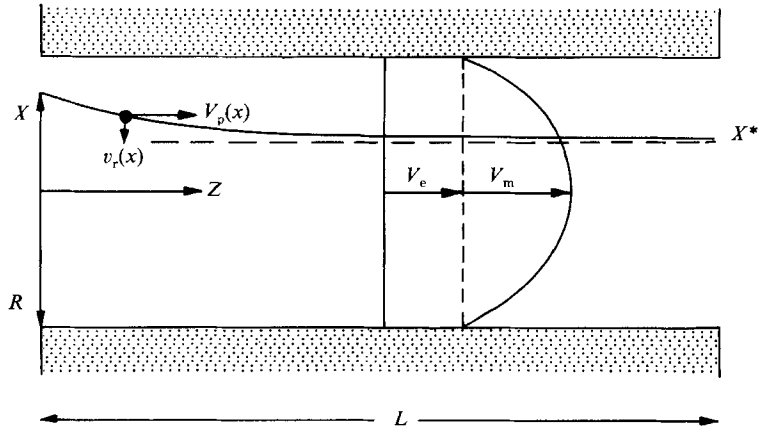

FIGURE 3. Flow through a pore (see the text).

An expression for $V_p(x)$ in combined Poiseuille and electrokinetic flow is

$$V_p(x) = \frac{dz}{dt} = V_m(1-x^2)(c_1 - c_2 x^5) + V_e. \tag{5}$$

The first term is the particle velocity in Poiseuille flow. It consists of the Poiseuille fluid velocity and a correction factor due to the finite particle size. In Poiseuille flow, the velocity of neutrally buoyant spheres is smaller than the fluid velocity at the centre of the sphere. The correction factor is based on experimental data by Goldsmith & Mason (1962) and we have given it a simple functional form by fitting their data to a polynomial in x. The coefficients c_1 and c_2 are

$$c_1 = 1 - \frac{2}{3}\left(\frac{b}{R}\right)^2, \quad c_2 = 23.36(1-c_1). \tag{6}$$

The maximum fluid velocity at the centre of the pore is given by

$$V_m = \frac{R^2 \Delta P}{4\eta L}, \tag{7}$$

where ΔP is the pressure drop across the pore length L.

The effect of radial migration is one of inertia. The radial force can exist with rigid particles only if the inertial effects, represented by the nonlinear terms in the Navier–Stokes equations, are included. Three empirical relationships proposed for the radial migration velocity (Segré & Silberberg 1962*b*; Jeffrey & Pearson 1965; Tachibana 1973) have been summarized in the same form (Ishii & Hasimoto 1980),

$$v_r(x) = \alpha\left(\frac{b}{R}\right)^2\left(\frac{\rho_f V_m^2 b}{4\eta}\right)x(x^*-x), \tag{8}$$

where α is a parameter associated with the strength of the rate of migration towards the equilibrium position x^* (see figure 3). The migration velocity depends strongly on particle size, pressure drop, and fluid viscosity. Segré & Silberberg (1962*b*) found that their equation adequately represented their data for pore Reynolds numbers up to 30. The later derivation by Ishii & Hasimoto (1980) is based on small pore Reynolds

numbers. In the present investigation, we have applied (8) for pore Reynolds numbers up to about one and obtained good agreement between theory and measurements.

Integration along a particle trajectory from a position $(x_0, z_0 = 0)$ at the pore entrance to a position (x, z) leads to the following expression,

$$\tilde{L} = \alpha l \left(\frac{b}{R}\right)^3 \left(\frac{\rho_f V_m}{4\eta}\right) = \int_{x_0}^{x} \frac{(1-x^2)(c_1 - c_2 x^5) + V_e/V_m}{x(x^* - x)} \mathrm{d}x, \tag{9}$$

where $l = z - z_0$ is the distance from the tube entrance and $\tilde{L}$ is a dimensionless measure of this distance. The above expression may be used to find the radial position a particle migrates to after having travelled through a pore of length L.

Owing to radial migration, the particle velocity in the z-direction will change as the particle migrates radially. By expressing $\mathrm{d}z$ in terms of $\mathrm{d}x$, the transit time is now found by intregrating (4) from the radial position x_0 at the pore inlet to the radial position x at the pore exit,

$$\tau = \frac{\beta}{V_m} \ln \frac{x(x^* - x_0)}{x_0(x^* - x)}, \tag{10}$$

where

$$\beta = \left[\alpha x^* \left(\frac{b}{R}\right)^3 \left(\frac{\rho_f V_m}{4\eta}\right)\right]^{-1}. \tag{11}$$

Equation (10) is valid only when the radial migration velocity is non-zero. Then, x is determined from (9) for a given x_0 and α. There exist two trajectories for which the migration velocity is zero. One is the trajectory for a particle entering at the pore axis and the other is the equilibrium trajectory. For these, the particle velocity $V_p(x)$ is independent of z and the particle transit time is easily determined. By measuring the minimum transit time (corresponding to $x = 0$) and the equilibrium transit time, the equilibrium position x^* is found by solving the corresponding seventh-degree equation in x. The minimum transit time is given by

$$\tau_{min} = \frac{\tau_0}{c_1 + V_e/V_m}, \tag{12}$$

where $\tau_0 = L/V_m$ is the minimum transit time for an infinite small particle in pure Poiseuille flow. The measured pressure and temperature (viscosity) cannot be expected to give exact agreement between the measured minimum transit time and the theoretical one. Experimental parameters in the theoretical expressions must be adjusted to obtain agreement. The starting point is always the measured minimum transit time and the equilibrium transit time. Equations (9) and (10) may then be combined to calculate the transit times for a single particle flowing back and forth through a pore. By comparing the experimental results with theory, an estimate for α is obtained.

4. Results and discussion

All experiments have been performed in horizontal pores at room temperature. The temperature variations during a series of experimental runs may have been about 0.5 °C. The pore Reynolds number has been low, ranging from 0.01 to 0.08 in the 3.1 μm diameter pore and about 1.3 for the experiments in the 27 and 30 μm diameter pores. The particle Reynolds number has been much smaller than one.

The fact that the particle enters and exits the pore at regular intervals, introduces additional effects that are not solely related to the motion of a particle in a very long

pore. Particle sedimentation and diffusion outside the pore in addition to entrance and exit effects are superimposed on the particle motion inside the pore. Effects that are small or negligible inside the pore, may be considerable outside the pore. For measurements using the large pores, particle sedimentation has been eliminated by density matching. For the small pore, this has not been necessary owing to the much smaller particle size used. Particle diffusion may perturb the reversibility of the particle motion outside the pore. The linear spread in position Δx for a particle due to diffusion is given by $\Delta x = (2\mathscr{D}t)^{\frac{1}{2}}$ (Einstein 1926), where $\mathscr{D}$ is the diffusion coefficient and t is the time the particle is allowed to diffuse. The diffusion coefficient is given by $\mathscr{D} = kT/6\pi\eta b$, where k is the Boltzmann constant and T the absolute temperature. Particle diffusion becomes an easily detectable effect for the 0.8 μm diameter spheres. The influence of entrance and exit effects has been studied by comparing particle migration in pores with different lengths.

When calculating transit times for comparison with measurements, particle diffusion has not been taken into account. A small component of diffusion is likely to introduce some stochasticity in the measured transit time series, but otherwise not seriously affect the measurements in any systematic manner. We assume that the particle re-enters the pore at the same radial position as it exits. The fractional radial coordinate where the particle first enters the pore is only approximately known and must be adjustable in the fitting procedure to find α. Here α determines how fast the particle reaches equilibrium and an estimate for α is obtained by finding the best overlap between the experimental transit time series and the theoretical one.

The minimum transit time has been determined from measurements of many (~ 1000) transit times of individual particles passing through the pore one at a time. To facilitate the presentation of the data, we define a normalized transit time τ_N which is equal to the transit time τ divided by the minimum transit time $\tau_{\min}$. A long transit time corresponds to a particle flowing close to the pore wall and a short transit time to a particle flowing close to the pore axis. The interval of possible transit times decreases with increasing particle size. When solid lines are used in plots to represent transit times, they are only defined at every passage through the pore. A sequence of measured or calculated transit times is a set of points and not a continuous function.

4.1. *A 27 and a 30 μm diameter pore*

4.1.1. *A neutrally buoyant particle*

The measurements to be reported below have been performed with neutrally buoyant 7.1 μm diameter spheres. We have mostly used a 27 μm diameter and 540 μm long pore, the pressure difference across the pore has been 1740 Pa, and the measured minimum transit time 4.8 ms. In order to investigate the importance of entrance and exit effects, similar measurements have also been performed using a 30 μm diameter and 315 μm long pore. Electrokinetic flow has been negligible compared to Poiseuille flow. The time between reversals has been 500 ms, during which a 7.1 μm diameter sphere diffuses of the order of 0.02 pore radii. Three typical examples of radial migration in the 27 μm diameter pore are shown in figure 4, which clearly illustrates migration away from the pore axis and wall towards equilibrium ($\tau^* = 6.2$ ms and $x^* = 0.46$). The measured transit times have been connected with solid lines and the first points have been emphasized with filled circles. One case is shown where a particle migrating away from the wall crosses the equilibrium position before eventually stabilizing. Such cases are quite frequent at all pressures, but perhaps increasingly so at small pressures. The other two measurements compare well with theory when α is close to one. The measured equilibrium position is in fair

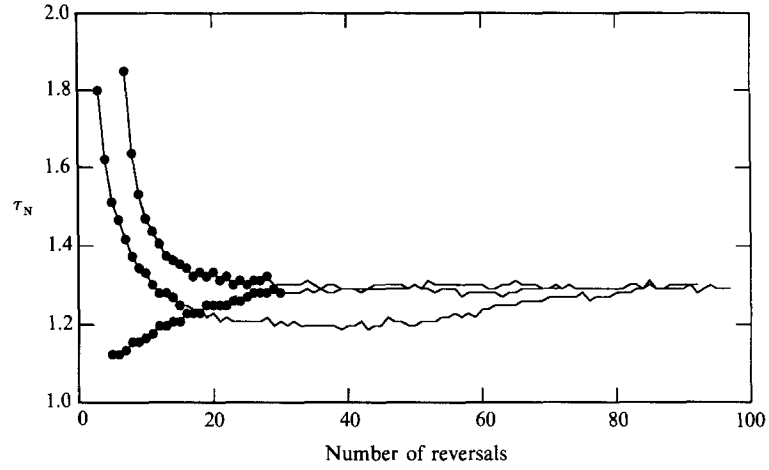

FIGURE 4. Three measurements, illustrating different routes towards the equilibrium position, of a 7.1 μm diameter sphere flowing back and forth through a 27 μm diameter and 540 μm long pore at $\Delta P = 1740$ Pa. The measured transit times have been connected with solid lines and the first points have been emphasized with filled circles ($\tau_{min} = 4.8$ ms, $\tau^* = 6.2$, and $x^* = 0.46$).

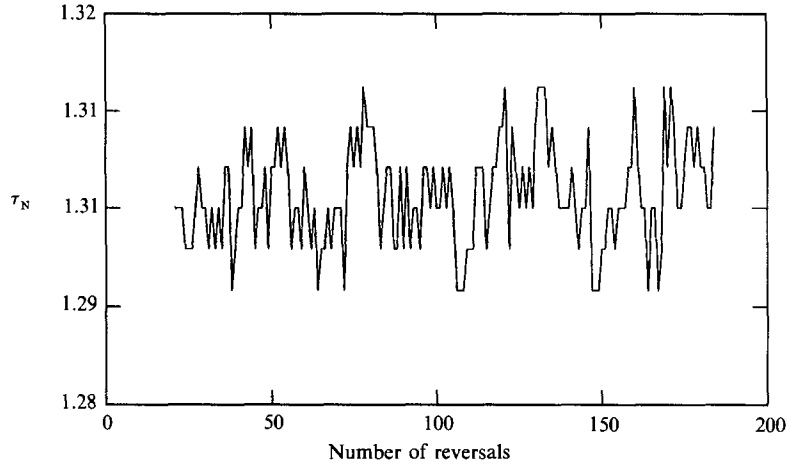

FIGURE 5. Normalized measured equilibrium transit times for a 7.1 μm diameter sphere flowing back and forth through a 27 μm diameter and 540 μm long pore at $\Delta P = 1740$ Pa ($\tau_{min} = 4.8$ ms, $\tau^* = 6.2$, and $x^* = 0.46$). The measured spread in τ^* corresponds to a radial displacement of only 0.15 μm.

agreement with measurements on the effect of particle size on the equilibrium position for neutrally buoyant systems investigated by Karnis *et al.* (1966). From their data, $x^* \approx 0.5$ for the same particle to pore diameter ratio. The equilibrium trajectory is found to be extremely stable as illustrated in figure 5 and we observe no time dependence in the equilibrium transit time. The calculated peak to peak spread in x^* is 0.011, which corresponds to a radial displacement of only 0.15 μm or 2% of the particle diameter. Thus, at equilibrium the particle retraces its path to a remarkable extent and the particle flow is effectively reversible. Possible deviations from reversibility are negligible and have not been accounted for. The measured fluctuations in τ^* may partly be due to particle diffusion outside the pore. Also, small pressure fluctuations may be a source of error. The time resolution of DATA 6000 was 20 μs, explaining the discrete steps in the plot.

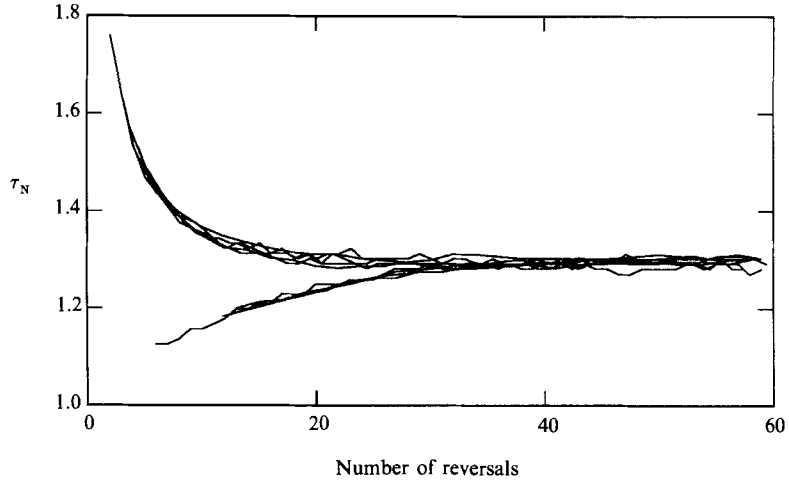

FIGURE 6. Radial migration of different 7.1 μm diameter spheres in a 27 μm diameter and 540 μm long pore at $\Delta P = 1740$ Pa approaching the equilibrium transit time ($\tau_{min} = 4.8$ ms, $\tau^* = 6.2$, and $x^* = 0.46$).

Different realizations are observed to have a small spread in the equilibrium transit times but otherwise overlap well. This is illustrated in figure 6 for measurements in the 27 μm diameter pore, which shows the overlap of 9 transit time series. The measurements were made during the same experimental run with the same experimental parameters. Figure 6 illustrates migration towards the equilibrium transit time $\tau^* = 6.2$ ms ($x^* = 0.46$). The data compare well with theory when $\alpha \approx 1$. In most cases, trajectories with the same minimum and equilibrium transit time overlap very nicely, but there are exceptions. Particles entering very close to the axis sometimes migrate much slower than expected and some have been observed to apparently stabilize close to the unstable equilibrium position $x^* = 0$. When a particle very close to the wall is captured and reversed, the first recorded transit time often corresponds to a much smaller migration velocity than the rest of the data indicate. This is interpreted as a result of interactions with the pore wall.

4.1.2. *Entrance and exit effects*

Convergent entrance and exit effects at positions remote from a meniscus have been investigated by Karnis & Mason (1967). For particles close to the wall, the outward displacement occurring at the exit was smaller than the corresponding inward movement at the entrance, while particles located closer to the axis passed into and out of the tube almost unhindered. If our system was to respond similarly, a slightly enhanced inward radial movement would be expected close to the wall. However, we find that particles entering very close to the wall have a smaller migration velocity than expected and this indicates that particle–pore interactions are more important than entrance and exit effects close to the wall. The effect of entrance and exit effects in our system has also been studied by comparing radial migration measurements using the 27 and 30 μm diameter pores, which differ in length by a factor 1.7 such that the number of reversals needed to reach equilibrium is significantly different. Radial migration measurements for particles entering close to the pore wall and axis are shown in figures 7 and 8, where a comparison has been made between the 540 μm long pore (plotted as filled circles) and the 315 μm long pore (plotted as open circles). In figure 8, only every second measured data point has

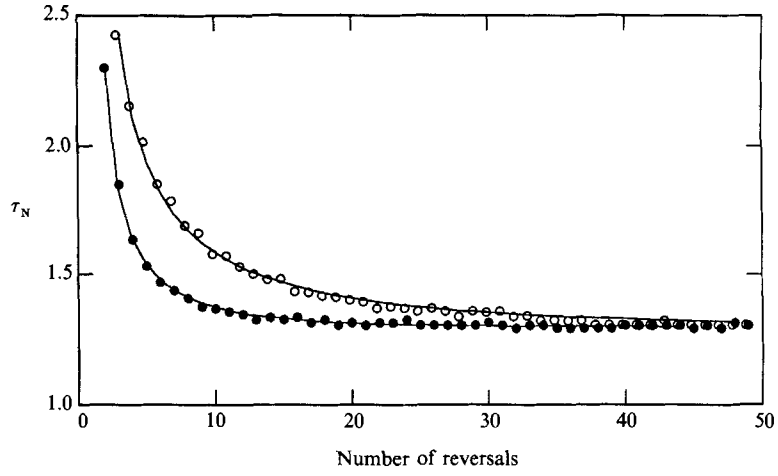

FIGURE 7. Radial migration of a 7.1 μm diameter sphere away from the pore wall for two different pore lengths. ●, 27 μm diameter and 540 μm long pore with $\Delta P = 1740$ Pa ($\tau_{min} = 4.8$ ms, $\tau^* = 6.2$, and $x^* = 0.46$), theory (solid curve): $\alpha = 1.06$; ○, 30 μm diameter and 315 μm long pore with $\Delta P = 720$ Pa ($\tau_{min} = 3.1$ ms, $\tau^* = 4.05$ ms, and $x^* = 0.47$), theory (solid curve): $\alpha = 1$.

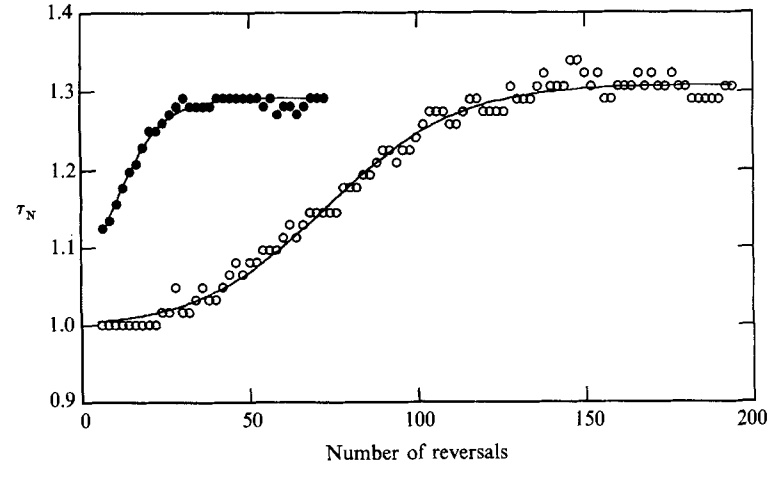

FIGURE 8. Radial migration of a 7.1 μm diameter sphere away from the pore axis for two different pore lengths. ●, 27 μm diameter and 540 μm long pore with $\Delta P = 1740$ Pa ($\tau_{min} = 4.8$ ms, $\tau^* = 6.2$, and $x^* = 0.46$), theory (solid curve): $\alpha = 1$; ○, 30 μm diameter and 315 μm long pore with $\Delta P = 720$ Pa ($\tau_{min} = 3.1$ ms, $\tau^* = 4.05$ ms, and $x^* = 0.47$), theory (solid curve): $\alpha = 1$.

been plotted for clarity. The fitted theoretical transit time series have been plotted as solid curves. The theoretical curve for the 540 μm long pore in figure 7 (corresponding to the filled circles) was calculated with $\alpha = 1.06$, the other three theoretical curves were calculated with $\alpha = 1$. The equilibrium position was approximately 0.46 pore radii from the axis. We note that the number of reversals to reach equilibrium increases when the pore length is shortened, as one would expect if radial migration is the major effect. Since we find practically the same value of α for both pore lengths, the observed radial movement of the particles is governed by the total pore length the particle has passed through and not by the number of exits. This confirms that the observed behaviour is due to radial migration and that entrance and exit effects are not significant for these pore lengths. Our system is

therefore a good approximation to studying migration in an infinitely long pore in this size range. The measured data scatter is probably related to particle diffusion outside the pore. Even with a small component of diffusion, we see that the radial particle movement is very distinct. The sphere migrating from the axis towards equilibrium in the 315 μm long pore (open circles in figure 8) moves a radial distance of about 7 μm during 150 reversals, which demonstrates the remarkable resolution our experimental setup offers.

4.1.3. *A non-neutrally buoyant particle*

A significant increase in the viscosity of the solution has a strong effect on the observed particle behaviour. The migration velocity inside the pore is then substantially reduced compared to sedimentation outside the pore. We enter into a regime with a great richness in observed effects, but where we lack a proper understanding of the various phenomena observed. The particle no longer stabilizes between the pore axis and the wall. It is instead carried to the pore wall by sedimentation outside the pore and eventually the particle is lost. This is illustrated in figure 9 for different 10 μm diameter polystyrene spheres flowing back and forth through a 27 μm diameter pore in a 52 wt % sucrose solution with 1 M NaCl. The solution is approximately twenty times more viscous than water and the pressure drop across the 540 μm long pore was 15200 Pa. The measured minimum transit time was 8.8 ms, in good agreement with the expected value. The spheres are almost 20 % less dense than the solution and they will rise. The figure illustrates how particles entering at different positions in the lower half of the pore cross-section rise mainly owing to buoyancy. Radial migration is now the perturbing effect and it is not strong enough to stabilize the particle at an equilibrium position. Note also the observed instability. The particle crosses the same radial coordinate twice more. This occurs close to the expected equilibrium position and it is probably the effect of radial migration almost balancing sedimentation. Roughly half of the measured trajectories are without this instability. The particles were reversed twice a second. The interplay between sedimentation outside the pore and radial migration inside the pore represents a challenge to theory and further experimental work is needed.

4.2. *A* 3.1 μm *diameter pore*

Radial migration has also been studied for 0.8 μm diameter spheres in a 3.1 μm diameter and 9.5 μm long pore. The temperature was 26 °C and the time between reversals was 250 ms for all measurements. The effect of sedimentation outside the pore is negligible while the particle may diffuse of the order of 0.25 pore radii while outside the pore. The transit time was recorded at every second passage through the pore, ensuring that the electrokinetic component of the transit time has the same sign for all recorded transit times. The pore voltage was 1.22 V, for which the transit time at zero pressure was approximately 16 ms.

Trajectories for 8 different 0.8 μm spheres migrating from the wall towards equilibrium are shown in figure 10. The pressure was 315 Pa and the measured minimum transit time 0.40 ms. Similar results were also obtained for 1 μm diameter spheres. The electrokinetic contribution to the transit time is only a few per cent and it has been neglected. Migration away from the wall is very distinct, but the individual particle trajectories are now more noisy and not necessarily monotonically decreasing. The equilibrium position is roughly 0.3 pore radii from the axis based on the data shown in figure 10. However, by considering a larger number of reversals, the average equilibrium position is found to be closer to the wall (see figure 11).

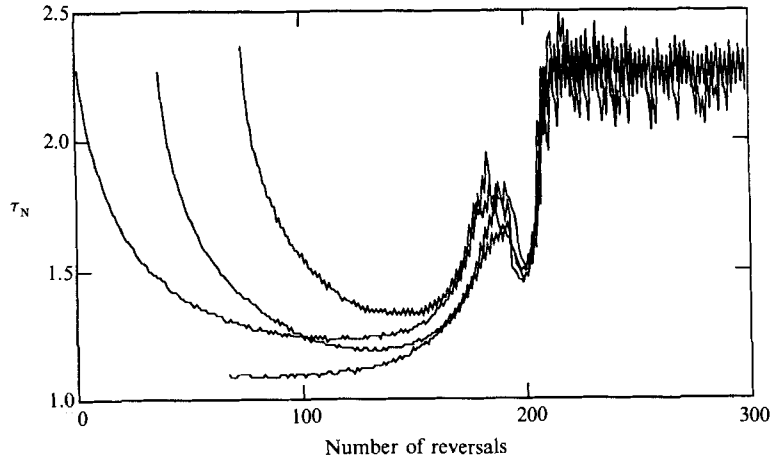

FIGURE 9. Normalized measured transit times for different 10 μm diameter spheres flowing back and forth through a 27 μm diameter and 540 μm long pore in a 52 wt % sucrose solution at ΔP = 15200 Pa. With observed instability.

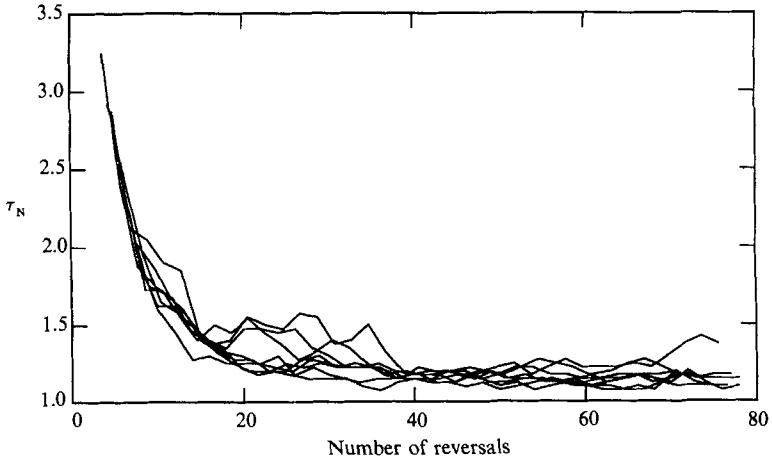

FIGURE 10. Radial migration of different 0.8 μm diameter spheres away from the pore wall in a 3.1 μm diameter and 9.5 μm long pore at ΔP = 315 Pa.

Migration outwards from the axis is not easily distinguished from fluctuations, while migration inwards from the wall is much easier to observe because migration then takes place over a large transit time interval.

It is now more difficult to fit a single experimental observation to theory, owing to the particle's more erratic path towards equilibrium. However, the average behaviour is still well accounted for by theory, $\alpha \approx 40$ compares very well with the measurements in figure 10, except for the longest transit times. Particles entering very close to the pore wall exhibit very long transit times, corresponding to minute migration velocities. Some transit times are even longer than we would expect without migration and we suspect this to be caused by interactions with the pore wall.

Even if migration is very distinct, also for submicron particles, the fluctuations in the equilibrium position are now considerable. We are in a regime where particle diffusion is important. Two measurements at different pressures are shown in figure

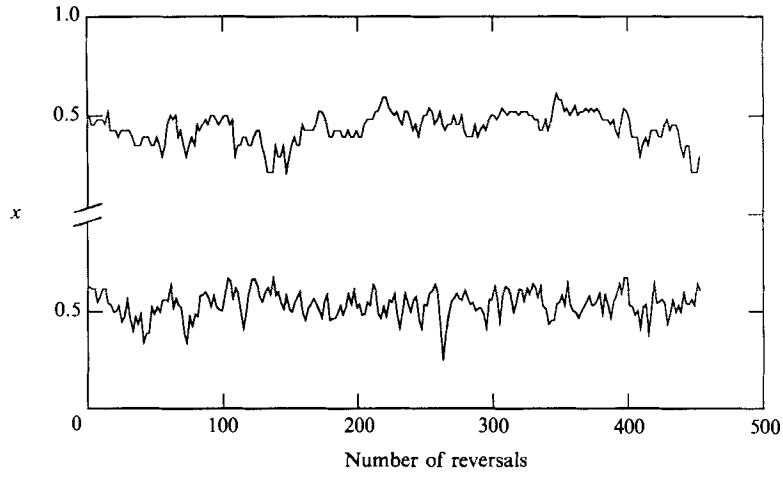

FIGURE 11. Variations in the equilibrium position for 0.8 μm diameter spheres in a 3.1 μm diameter and 9.5 μm long pore at $\Delta P = 105$ Pa (lower curve) and $\Delta P = 570$ Pa (upper curve).

11. The equilibrium transit times were measured at every second reversal and they have been transformed into the equivalent radial positions. The electrokinetic flow was in the same direction as the Poiseuille flow. For the lower curve, the pressure drop was 105 Pa, the minimum transit time 1.2 ms, and the average equilibrium transit time 1.7 ms ($x^* = 0.55$). The corresponding values for the upper curve are 570 Pa, 0.21 ms, and 0.27 ms ($x^* = 0.44$). Also measurements in the large pores indicate that the equilibrium position is shifted closer to the wall when the pressure is lowered. Electrokinetic flow is negligible at the high pressure, while at the low pressure, $V_e = 0.03 V_m$. Comparing the two curves in figure 11, the standard deviation of the radial distance between neighbouring sites is 0.046 pore radii for the upper curve and 0.068 pore radii for the lower curve. Hence, at the low pressure, the radial displacement during consecutive reversals is roughly 50% larger than at the high pressure. Two things change when the pressure is lowered. The particle transit time increases and consequently the fluctuations in the radial position, owing to transverse diffusion inside the pore, increase. Next, the radial migration velocity is proportional to the pressure squared and decreases when the pressure is lowered. The tendency to bring particles back to equilibrium is therefore much smaller at the lower pressure and the fluctuations will be less damped. Both increased diffusion inside the pore and less radial migration, make allowance for increased fluctuations in the radial position when the pressure is decreased, in accordance with our observations.

5. Concluding remarks

Radial migration of polystyrene spheres smaller than 10 μm in diameter has been studied by the resistive pulse technique combined with our new pressure reversal technique. Migration towards the off-axis equilibrium position from both the pore axis and the wall have been observed. Equivalent realizations under the same experimental conditions are almost identical and individual trajectories compare well with theory. Additional effects to radial migration are entrance and exit effects, sedimentation, and diffusion. The influence of entrance and exit effects have been shown to be of little importance for the 27 and 30 μm diameter pores. The rate at which a particle in a long pore reaches equilibrium is primarily determined by the

total pore length the particle has passed through and not by the number of times it enters and exits the pore. For neutrally buoyant 7.1 μm diameter spheres, the equilibrium position is extremely stable and the particle flow is effectively reversible. When particle sedimentation outside the pore becomes significant (by using a 52 wt % sucrose solution), sedimentation dominates and there is no longer a stable equilibrium position. For the 3.1 μm diameter pore, particle diffusion is an important effect. The equilibrium transit time fluctuates strongly but we still observe very distinct migration inwards from the wall. It is assumed that the fluctuations are related mainly to particle diffusion outside the pore affecting the radial position at which the particle re-enters the pore. The particle displacement increases when the migration velocity decreases (by lowering the pressure drop across the pore).

Our measurements have been performed in very small systems and the viscosity has been close to that of water, while in previous work, experiments have been carried out in much larger systems using fluids with higher viscosities. Our values of α for the strength of the rate of migration are in good agreement with values obtained by Segré & Silberberg (1962*b*), Jeffrey & Pearson (1965) and Tachibana (1973), whose values of α are in the range 0.90–9.1. Their equilibrium positions were 0.63, 0.68, and 0.60, respectively, while our measured equilibrium positions are closer to the axis ($x^* \approx 0.46$). This may be explained by our larger particle to pore diameter ratio. For the 27 and 30 μm diameter pores we obtained α-values very close to one. The 3.1 μm diameter pore gives larger values, $\alpha \approx 40$.

Our system may be considered as a one-dimensional porous medium with only one pore size. Phenomena occurring inside and outside the pore may be studied in detail. Information on individual effects is attainable by choosing suitable experimental conditions. The interaction between different physical processes may be studied under well-defined conditions. This study has focused on radial migration, but the richness in observed effects justifies continued efforts in this field to obtain a better understanding of the flow behaviour due to the combined effect of several physical processes. The pressure reversal technique gives access to a size range which is not well covered by other techniques and we have been able to study a nonlinear hydrodynamic effect on the pore level with great accuracy. This paper has laid a foundation for studies of particle flow dynamics in very small systems and it has revealed a new potential of the resistive pulse technique.

The author would like to thank Professors J. Feder and T. Jøssang for encouragement and many very useful discussions. Dr R. W. DeBlois has kindly given me 3 μm diameter pores. P. Hatlestad has skilfully constructed the electronics needed and his assistance is greatly appreciated. The financial support of Den Norske Stats Oljeselskap A.S. (Statoil) is gratefully acknowledged.

REFERENCES

Aoki, H., Kurosaki, Y. & Anzai, H. 1979 Study on the tubular pinch effect in a pipe flow. I. Lateral migration of a single particle in laminar Poiseuille flow. *Bull. JSME* **22**, 206.

Berge, L. I., Feder, J. & Jøssang, T. 1989 A novel method to study single-particle dynamics by the resistive pulse technique. *Rev. Sci. Instrum.* **60**, 2756.

Brenner, H. 1966 Hydrodynamic resistance of particles at small Reynolds numbers. *Adv. Chem. Engng* **6**, 287.

Brenner, H. & Happel, J. 1958 Slow viscous flow past a sphere in a cylindrical tube. *J. Fluid Mech.* **4**, 195.

BRETHERTON, F. P. 1962 The motion of rigid particles in a shear flow at low Reynolds number. *J. Fluid Mech.* **14**, 284.

COULTER, W. H. 1953 US Patent No. 2656508.

DEBLOIS, R. W. & BEAN, C. P. 1970 Counting and sizing of submicron particles by the resistive pulse technique. *Rev. Sci. Instrum.* **41**, 909.

DEBLOIS, R. W., BEAN, C. P. & WESLEY, R. K. A. 1977 Electrokinetic measurements with submicron particles and pores by the resistive pulse technique. *J. Colloid Interface Sci.* **61**, 323.

DUKHIN, S. S. 1974 Development of notions as to the mechanism of electrokinetic phenomena and the structure of the colloid micelle. In *Surface and Colloid Science*, vol. 7 (ed. E. Matijević), pp. 1–47. Wiley.

EINSTEIN, A. 1926 *Theory of Brownian Movement*. Methuen.

FISCHER, B. E. & SPOHR, R. 1983 Production and use of nuclear tracks: imprinting structure on solids. *Rev. Mod. Phys.* **55**, 907.

GOLDSMITH, H. L. & MASON, S. G. 1962 The flow of suspensions through tubes. I. Single spheres, rods, and discs. *J. Colloid Sci.* **17**, 448.

ISHII, K. & HASIMOTO, H. 1980 Lateral migration of a spherical particle in flows in a circular tube. *J. Phys. Soc. Japan* **48**, 2144.

JEFFREY, R. C. & PEARSON, J. R. A. 1965 Particle motion in laminar vertical tube flow. *J. Fluid Mech.* **22**, 721.

KARNIS, A., GOLDSMITH, H. L. & MASON, S. G. 1966 The flow of suspensions through tubes. V. Inertial effects. *Can. J. Chem. Engng* **44**, 181.

KARNIS, A. & MASON, S. G. 1967 The flow of suspensions through tubes. VI. Meniscus effects. *J. Colloid Interface Sci.* **23**, 120.

MAXWELL, J. C. 1904 *A Treatise on Electricity and Magnetism*, 3rd edn, vol. 1. Clarendon.

OLIVER, D. R. 1962 Influence of particle rotation on radial migration in the Poiseuille flow of suspensions. *Nature* **194**, 1269.

RUBINOW, S. I. & KELLER, J. B. 1961 The transverse force on a spinning sphere moving in a viscous fluid. *J. Fluid Mech.* **11**, 447.

SAFFMAN, P. G. 1956 On the motion of small spheroidal particles in a viscous liquid. *J. Fluid Mech.* **1**, 540.

SAFFMAN, P. G. 1965 The lift on a small sphere in a slow shear flow. *J. Fluid Mech.* **22**, 385.

SEGRÉ, G. & SILBERBERG, A. 1962*a* Behaviour of macroscopic rigid spheres in Poiseuille flow. Part 1. Determination of local concentration by statistical analysis of particle passages through crossed light beams. *J. Fluid Mech.* **14**, 115.

SEGRÉ, G. & SILBERBERG, A. 1962*b* Behaviour of macroscopic rigid spheres in Poiseuille flow. Part 2. Experimental results and interpretation. *J. Fluid Mech.* **14**, 136.

SMITH, A. M. O. 1960 Remarks on transition in a round tube. *J. Fluid Mech.* **7**, 565.

SMYTHE, W. R. 1964 Flow around a spheroid in a circular tube. *Phys. Fluids* **7**, 633.

TACHIBANA, M. 1973 On the behaviour of a sphere in the laminar tube flows. *Rheol. Acta* **12**, 58.